2023 IEEE/ASME International Conference on Advanced Intelligent Mechatronics (AIM)
June 28-30, 2023. Seattle, Washington, USA

# Six-bar Pulley-Guided Node Based Prismatic Tensegrity Robot Form-finding Analysis and Experiment

Azamat Yeshmukhametov, Aisulu Tileukulova, and Koichi Koganezawa

***Abstract*—This study offers a unique analysis of node-based tensegrity robots guided by pulleys. Tensegrity structures comprise some compressive and tensile members, which provide a lightweight and flexible body. The primary goal of this research is to show how reducing friction in tensegrity robots through the use of pulley-guided nodes can enhance their form-finding capabilities, as demonstrated by experimental evidence. The proposed new pulley-based node design reduces friction between wires and rigid components, thereby improving the form-finding ability of the robots.**

***Index Terms*—Tensegrity, robot design, pulley-guided node, form-finding analysis**

## I. INTRODUCTION

A unique and innovative type of robotic design, known as tensegrity robots, draws inspiration from the tensegrity structures present in the natural world [1], [2]. These robots merge the principles of tension and compression elements to form a highly stable structure that can adapt to dynamic environments. Tensegrity robots are recognized for their ability to efficiently handle impacts, maintain balance, and traverse challenging terrains [3]. With their innovative design and adaptable capabilities, tensegrity robots have the potential to revolutionize the field of robotics [4].

Tensegrity robots come in a variety of forms, each with unique capabilities and constraints. The cable-driven tensegrity robot, which uses a network of cables to transmit tension throughout the robot, is one of the most popular varieties [5]. These machines typically weigh little and have a wide range of motion, which makes them ideal for jobs that call for quickness and agility. Pneumatic tensegrity robots are another variety of tensegrity robots, which use air pressure to regulate their shape and motion. These robots are extremely adaptable and can be programmed to carry out a variety of tasks [6], from straightforward repetition to intricate manipulation.

Tensegrity robots have several unique capabilities that make them well-suited for a variety of applications. One of the key features of tensegrity robots is their ability to withstand significant deformation without breaking, making them highly resilient to damage [7]. This makes them ideal for use in harsh environments, such as in space exploration or disaster response [8]. Tensegrity robots are also known for their ability to efficiently handle impacts, making them well-suited for tasks that involve jumping or landing [9], [10].

Another advantage of tensegrity robots is their ability to maintain balance and stability, even on uneven terrain [6], [11]–[15]. This makes them well-suited for tasks that involve traversing rough terrains, such as search and rescue missions. Tensegrity robots also have the ability to perform multiple tasks simultaneously, making them well-suited for tasks that require coordination between multiple parts of the robot.

Despite their many advantages, tensegrity robots also have some limitations. One of the biggest challenges in designing tensegrity robots is finding the right balance between stability and flexibility [16]. The tension and compression elements must be carefully designed to ensure that the robot remains stable while also allowing for adequate movement [17]. Another challenge is the control of tensegrity robots, as the combination of tension and compression elements can make it difficult to predict how the robot will respond to different inputs [18].

Tensegrity form-finding and stability analysis are critical steps in tensegrity structure design and optimization. Form-finding is the process of determining the optimal configuration of a structure for a given load condition while taking the structure's stiffness and geometry into account [15]. As it is mentioned above, wire-driven robot transmission mostly suffers from the friction effect and high torque demand [19], therefore, pulley-guided or idlers are necessary in case of effective and smooth motion transmission [20]. In tensegrity robots, form-finding is critical for determining the most efficient and stable structure for a given set of requirements. Stability analysis, on the other hand, entails investigating the structure's behavior under external loads and environmental conditions [16]. The stability analysis considers the structure's dynamic response to external loads and evaluates structural stability and safety margins. The results of the stability analysis provide important information for the design and optimization of tensegrity structures and can be used to identify critical load conditions and modes of failure [21]. The combination of form-finding and stability analysis allows for a comprehensive assessment of the performance of tensegrity structures and enables the optimization of their design for specific applications. The development of efficient form-finding and stability analysis

This work was supported by Nazarbayev University under a social grant.

A. Yeshmukhametov is with the Department of Robotics Engineering, School of Engineering and Digital Sciences, Nazarbayev University, Astana, Kazakhstan. yeshmukhametov.coba@gmail.com

A. Tileukulova is with the Department of Physics and Technology, Al-Farabi Kazakh National University, Almaty, Kazakhstan. Email: aisulu.tileukulova@gmail.com

K. Koganezawa is with the Department of Mechanical Engineering, Tokai University, Hiratsuka, Kanagawa, Japan. Email: kogane@keyaki.cc.u-tokai.ac.jp

methods is essential for the advancement of tensegrity structures and their applications in engineering [22].

In this study, we present a new pulley-guided nodes-based prismatic tensegrity robot form-finding analysis. The paper is structured as follows: Design concept, Initial posture calibration, form-finding experiment analysis, results, and conclusion.

## II. Design Concept

The proposed stiffness formula in this study is specifically developed for the analysis of prismatic tensegrity structures. These structures are characterized by a fixed base and a movable top plate having a polyhedral shape, which allows for greater versatility in their applications. The superior load-bearing capacity of prismatic tensegrity structures is attributed to the efficient distribution of applied loads throughout the structure, facilitated by the use of saddle wires weaved in a polyhedral shape as well. The present study focuses on tensegrity structures composed of three active wires, connected to motors, three passive wires, anchored to tension springs to provide stiffness and rigidity, and a saddle wire to maintain symmetrical balance in the structure. The proposed stiffness formula provides a comprehensive method for quantifying the stiffness and stability of prismatic tensegrity structures, contributing to the advancement of their design and optimization in various engineering applications (see figure 1).

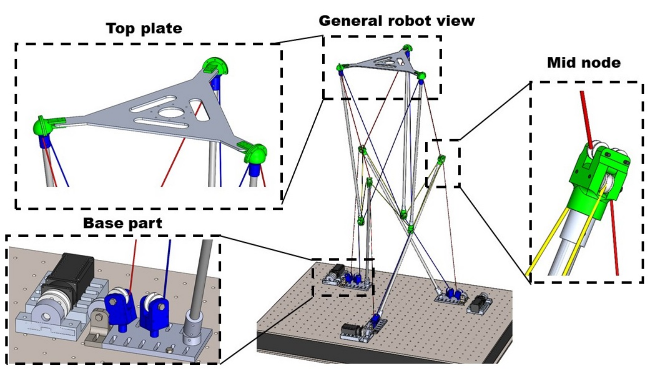


Fig. 1. Polyhedral tensegrity robot CAD design concept

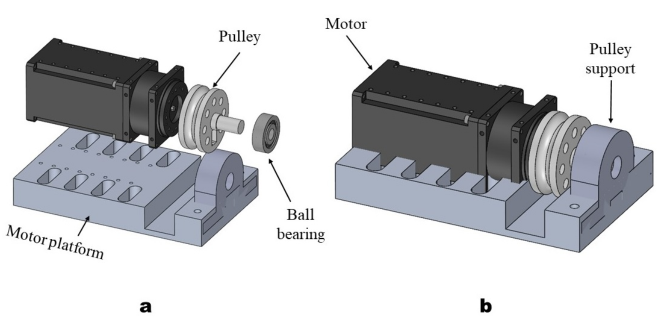


Fig. 2. Tensegrity robot actuation unit a) Exploded view b) Assembled view

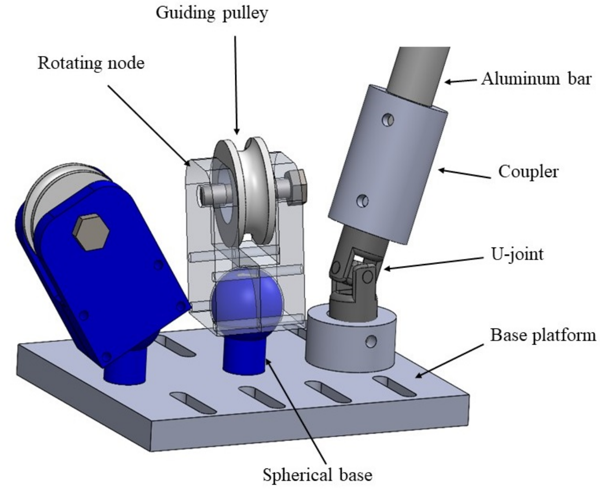


Fig. 3. Tensegrity robot base node design

### A. Tensegrity robot base node and actuation unit

The tensegrity robot is driven by three servo motors via directly connected pulleys. In order to give the motors a stable working and torque holding, we developed a ball-bearing pulley holder in the drive unit that maintains a high tension in the output ( see figure 2). In wire-driven mechanisms, one of the major challenges is derailing the wire from the pulley groove. Therefore, in this research work, we have designed base nodes with self-aligning properties using spherical joints. The design provides better driving work of the wire and prevents derailing of the wire (see figure 3 ).

Another advantage of using pulley-guided nodes is their ability to maintain static equilibrium. This is because a tensegrity structure is a network of wires that form a closed web, so a change in tension in one wire can affect the entire structure. By using pulley-guided nodes, external forces are distributed evenly throughout the structure, allowing the wire tension to be controlled by the applied load.

### B. Tensegrity nodes design

One challenge in designing tensegrity structures is friction between the wires and rigid components of the robot. To address this issue, this robot has middle nodes equipped with guide rollers to reduce friction and ensure smooth wire guidance and movement. As a result, the form-finding capabilities of the tensegrity structure are significantly improved. (figure 4).

The self-alignment of wires extends the lifespan of the robot's components and enhances the repeatability of the robot's motion. The middle notes are fitted with linear bearings normally used for sliding along Z-axis, although it allows rotation. The reviewer will wonder if the nodes have prismatic DOF. The upper node design features a spherical joint with eyelets for mounting both active and passive wires.

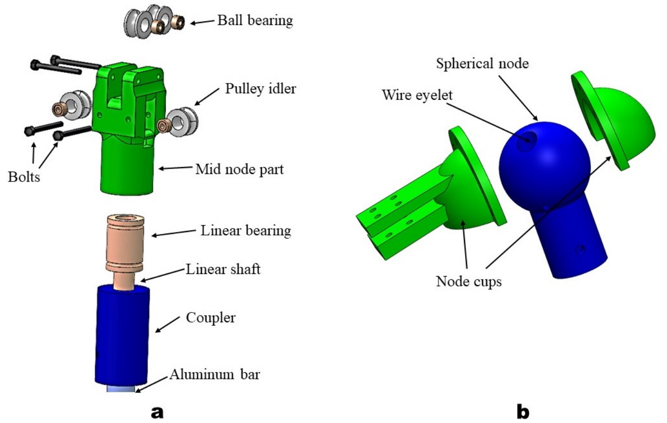


Fig. 4. Tensegrity robot actuation unit a) Mid node design b) Upper node design

## III. INITIAL POSTURE CALIBRATION

Tensegrity robot arm initial posture calibration is one of the key points to control. In this prototype, we use three types of wires: active, passive, and saddle wires. The active wires are directly connected to the motors to actuate the robot, the passive wires are connected to the extension springs for providing rigidity to the robot structure, and the saddle wire takes a role to sustain the weight of the upper layer and to take a kinetic balance of the whole structure. So, the robot's shape and form depend on wire tension. To measure wire tension values, we install seven tension sensors (Flintec Y1) along all wires, three sensors for driving wires, three for passive wires, and one for the saddle wire (figure 5).

The analog output of the tension sensor goes to the amplifier module and the amplified signal goes to the A/D converting pins of the microcontroller. Obtained signals are visualized and analyzed in the ROS environment. The proper calibration operation is achieved by using sensor data. There are two main conditions in the calibration of the tensegrity robot's initial posture:

1. The line between the upper plate and base plate centers should be aligned on a vertical line. In addition, the upper plate should be on a horizontal plane.
2. The tension accumulation of wires in each upper plate node should be equal.

$$T_{21} = S_{a1} + S_{p1}, T_{22} = S_{a2} + S_{p2}, T_{23} = S_{a3} + S_{p3}$$
$$T_{21} \cong T_{22} \cong T_{23}$$

Here $T_{21}, T_{22}, T_{23}$ are sum of wire tension values in $n_{21}, n_{22}, n_{23}$ nodes respectively. Active wires $S_{a1}, S_{a2}, S_{a3}$, passive wires $S_{p1}, S_{p2}, S_{p3}$ (figure 6). To prove this concept, we utilized seven wire tension sensors Flintec along the wires and measured wire tension in case of motion and in the standby state.

The plot in Figure 7 clearly displays the second condition of tensegrity posture calibration, as evident from the data presented.

## IV. FORM-FINDING EXPERIMENT ANALYSIS

To prove the concept of robot form-finding capability, we run the robot in a circular trajectory along the z-axis. Then tracked by cameras to capture the motion trajectory with markers. According to the definition of the tensegrity form-finding feature, the robot should return to its original or initial posture after performing a certain motion trajectory. In this experiment, we utilized Optitrack motion capture cameras to gather data on the motion of the robot (figure 8). The objective of the experiment was to evaluate the form-finding capabilities of the tensegrity structure after a specific moving trajectory. Based on Optitrack datasheet documentation, the maximum deviation error of the marker's capture precision is around 0.4mm.

In this experiment, we integrated the control program, commands, and sensors into the Robot Operating System (ROS) environment. The experiment was conducted using two computers with different operating systems: Ubuntu and Windows, with the ROS system operating on Ubuntu. Circular motion commands were transmitted to the Dynamixel motors through the ROS, while the motion capture system monitored the markers attached to the tensegrity nodes (see figure 9. In our study, we introduced a novel kinematic approach that utilizes a constrained kinematic and kinetic model [23]. Tensegrity structures are widely recognized for their hyper-redundancy, which makes it challenging to achieve a desired end-effector position. To overcome this challenge, we established mathematical constraints to restrict superfluous movements while preserving essential ones.

## V. EXPERIMENT

To validate the benefits of pulley-guided nodes in comparison to traditional tensegrity nodes, wire tension sensors were installed along the saddle wire at the connection points of each node. In this experiment, six sections were analyzed and six sensors were utilized, as shown in Figure 7. It is worth noting that the non-pulley guided node design is susceptible to significant friction between the wire and the robot's rigid components, resulting in reduced efficiency. On the other hand, the pulley-guided design significantly minimizes friction, enabling the wire to move freely and the robot to operate smoothly.

The experiment, as depicted in Figure 9, involved using ROS to control the robot's motors and follow a sinusoidal trajectory (as shown in Figure 10). The objective was to evaluate the initial and final postures of the robot and accurately determine the node positions after two circular motions along the z-axis, followed by a return to the initial posture. Using data obtained from OptiTrack, the form-finding discrepancy was determined.

According to table I the nodes' position before and after the motion experiment is almost identical. In this research, we measured all 12 nodes' trajectory, initial and final positions (see figure) 11. As regards, discrepancy of nodes' position, mostly occurs in the middle nodes, because markers of the middle nodes are located inner side of the tensegrity and

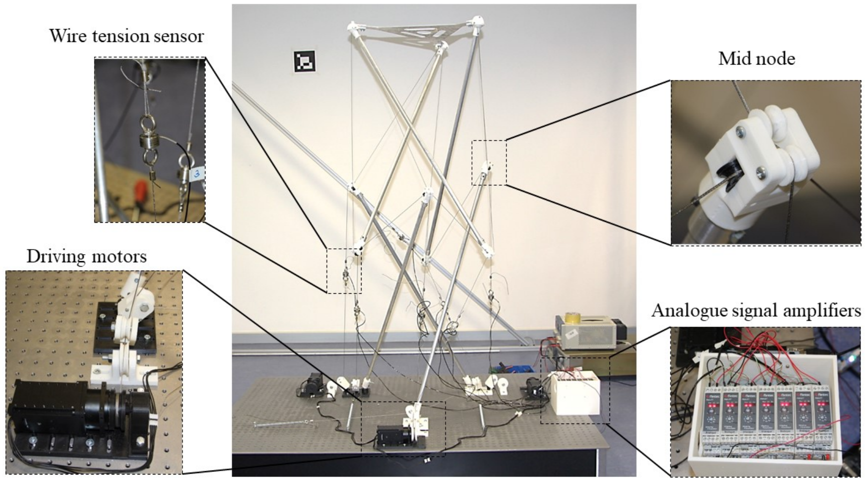


Fig. 5. Tensegrity robot experimental prototype

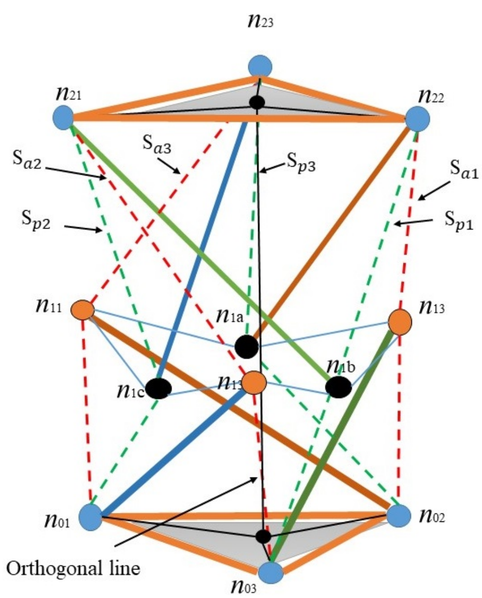


Fig. 6. Tensegrity robot structure notation for calibration

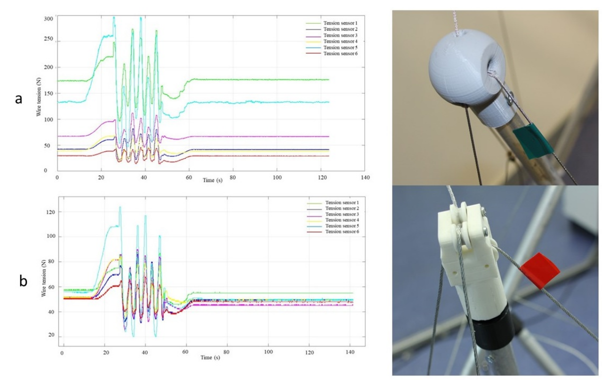


Fig. 7. Wire tension value difference in case of circular motion, a) Non-pulley guided node design b) fully pulley guided node design

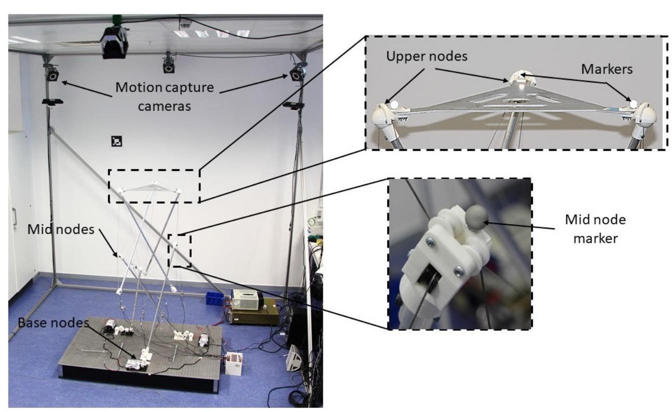


Fig. 8. Experimental setup and preparation

during the motion, some cameras could not see the markers at a certain time.

## VI. Conclusion

In conclusion, this research aimed to study the form-finding feature of a tensegrity robot through an experimental analysis based on a proposed stiffness formulation. The results, as shown in Table 1, indicate that the robot was able to return to its initial position with high precision, with an error rate of less than 1 percent. However, it should be noted that the experiment did not evaluate the repeatability of the tensegrity structure. As a next step, the researchers plan to investigate the repeatability of the form-finding feature and the effect of friction on the

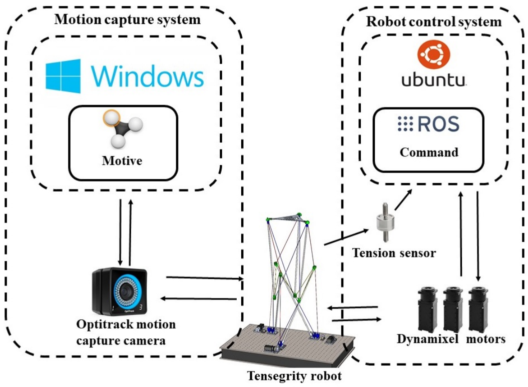


Fig. 9. Experimental environment

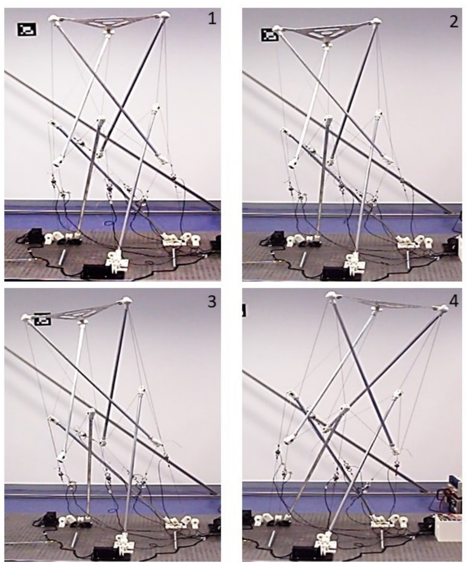


Fig. 10. Tensegrity robot circular motion captures

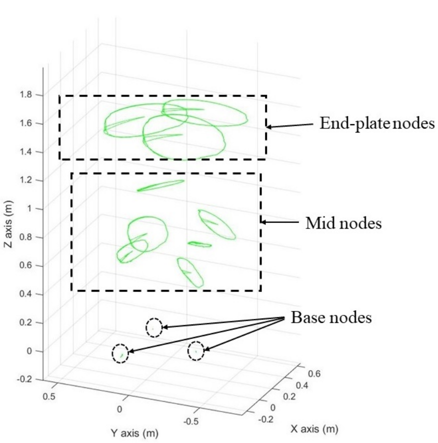


Fig. 11. Tensegrity robot nodes motion trajectory

TABLE I
TENSEGRITY ROBOT INITIAL AND FINAL NODES POSITION.

| | Nodes | Initial pos | | | Final pos | | |
|---|---|---|---|---|---|---|---|
| | | X (mm) | Y (mm) | Z (mm) | X (mm) | Y (mm) | Z (mm) |
| Base plate | $n_{01}$ | 250 | 0 | 0 | 250 | 0 | 0 |
| | $n_{02}$ | -130 | -225 | 0 | -130 | -225 | 0 |
| | $n_{03}$ | -130 | 225 | 0 | -130 | 225 | 0 |
| Mid nodes | $n_{11}$ | 144 | 50 | 920 | 144 | 50 | 920 |
| | $n_{12}$ | -50 | -150 | 920 | -50 | -150 | 920 |
| | $n_{13}$ | -130 | 110 | 910 | -130 | 110 | 910 |
| | $n_{1a}$ | 125 | -70 | 673 | 115 | -70 | 673 |
| | $n_{1b}$ | 135 | -70 | 662 | 135 | -69 | 663 |
| | $n_{1c}$ | -14 | 150 | 671 | -14 | 150 | 671 |
| Upper plate | $n_{21}$ | 18 | 257 | 1590 | 18 | 257 | 1590 |
| | $n_{22}$ | -250 | -104 | 1600 | -250 | -104 | 1600 |
| | $n_{23}$ | 197 | -156 | 1600 | 197 | -156 | 1600 |

structure. Moreover, investigate impact of friction effect to the robot payload capacity and manipulability.

## REFERENCES

[1] M. Masic, R. E. Skelton, and P. E. Gill, "Optimization of tensegrity structures," *International Journal of Solids and Structures*, vol. 43, no. 16, pp. 4687–4703, 2006.

[2] J. Zhang and M. Ohsaki, "Stability conditions for tensegrity structures," *International Journal of Solids and Structures*, vol. 44, no. 11, pp. 3875–3886, 2007. [Online]. Available: https://www.sciencedirect.com/science/article/pii/S002076830600446X

[3] Q. Zhang, D. Zhang, Y. Dobah, F. Scarpa, F. Fraternali, and R. E. Skelton, "Tensegrity cell mechanical metamaterial with metal rubber," *Applied Physics Letters*, vol. 113, no. 3, p. 031906, 2018.

[4] A. P. Sabelhaus, J. Bruce, K. Caluwaerts, P. Manovi, R. F. Firoozi, S. Dobi, A. M. Agogino, and V. SunSpiral, "System design and locomotion of SUPERball, an untethered tensegrity robot," in *IEEE International Conference on Robotics and Automation (ICRA)*, 2015, pp. 2867–2873.

[5] S. Faroughi, H. H. Khodaparast, and M. I. Friswell, "Non-linear dynamic analysis of tensegrity structures using a co-rotational method," *International Journal of Non-Linear Mechanics*, vol. 69, pp. 55–65, 2015. [Online]. Available: https://www.sciencedirect.com/science/article/pii/S0020746214002376

[6] S. H. Juan and J. M. Mirats Tur, "Tensegrity frameworks: Static analysis review," *Mechanism and Machine Theory*, vol. 43, no. 7, pp. 859–881, 2008. [Online]. Available: https://www.sciencedirect.com/science/article/pii/S0094114X07001218

[7] M. Lacagnina, S. Russo, and R. Sinatra, "A novel parallel manipulator architecture for manufacturing applications," *Multibody System Dynamics*, vol. 10, no. 2, pp. 219–238, 2003.

[8] S. F. Assal, "Self-organizing approach for learning the forward kinematic multiple solutions of parallel manipulators," *Robotica*, vol. 30, no. 6, pp. 951–961, 2012.

[9] S. Liu, Q. Li, P. Wang, and F. Guo, "Kinematic and static analysis of a novel tensegrity robot," *Mechanism and Machine Theory*, vol. 149, p. 103788, 2020.

[10] M. Arsenault and C. M. Gosselin, "Kinematic and static analysis of a 3-pups spatial tensegrity mechanism," *Mechanism and Machine Theory*, vol. 44, no. 1, pp. 162–179, 2009.

[11] L. Zhang, B. Maurin, and R. Motro, "Form-finding of nonregular tensegrity systems," *Journal of Structural Engineering*, vol. 132, no. 9, pp. 1435–1440, 2006.

[12] M. Yamamoto, B. Gan, K. Fujita, and J. Kurokawa, "A genetic algorithm based form-finding for tensegrity structure," *Procedia Engineering*, vol. 14, pp. 2949–2956, 2011, east Asia-Pacific Conference on Structural Engineering and Construction. [Online]. Available: https://www.sciencedirect.com/science/article/pii/S1877705811014482

[13] K. Koohestani, "Form-finding of tensegrity structures via genetic algorithm," *International Journal of Solids and Structures*, vol. 49, no. 5, pp. 739–747, 2012. [Online]. Available: https://www.sciencedirect.com/science/article/pii/S0020768311003970

[14] M. Pagitz and J. Mirats Tur, "Finite element based form-finding algorithm for tensegrity structures," *International Journal of Solids and Structures*, vol. 46, no. 17, pp. 3235–3240, 2009. [Online]. Available: https://www.sciencedirect.com/science/article/pii/S0020768309001802
[15] G. G. Estrada, H.-J. Bungartz, and C. Mohrdieck, "Numerical form-finding of tensegrity structures," *International Journal of Solids and Structures*, vol. 43, no. 22, pp. 6855–6868, 2006. [Online]. Available: https://www.sciencedirect.com/science/article/pii/S0020768306000448
[16] A. Tibert and S. Pellegrino, "Review of form-finding methods for tensegrity structures," *International Journal of Space Structures*, vol. 18, no. 4, pp. 209–223, 2003.
[17] H. Murakami, "Static and dynamic analyses of tensegrity structures. part 1. nonlinear equations of motion," *International Journal of Solids and Structures*, vol. 38, no. 20, pp. 3599–3613, 2001. [Online]. Available: https://www.sciencedirect.com/science/article/pii/S0020768300002328
[18] C. Sultan, M. Corless, and R. E. Skelton, "Linear dynamics of tensegrity structures," *Engineering Structures*, vol. 24, no. 6, pp. 671–685, 2002. [Online]. Available: https://www.sciencedirect.com/science/article/pii/S0141029601001304
[19] A. N. Yeshmukhametov, K. Koganezawa, Z. Buribayev, Y. Amirgaliyev, and Y. Yamamoto, "Study on multi-section continuum robot wire-tension feedback control and load manipulability," *Industrial Robot: the international journal of robotics research and application*, vol. 47, no. 6, pp. 837–845, 2020.
[20] A. Yeshmukhametov, K. Koganezawa, A. Seidakhmet, and Y. Yamamoto, "Wire-tension feedback control for continuum manipulator to improve load manipulability feature," in *2020 IEEE/ASME International Conference on Advanced Intelligent Mechatronics (AIM)*. IEEE, 2020, pp. 460–465.
[21] R. E. Skelton, R. Montuori, and V. Pecoraro, "Globally stable minimal mass compressive tensegrity structures," *Composite Structures*, vol. 141, pp. 346–354, 2016. [Online]. Available: https://www.sciencedirect.com/science/article/pii/S0263822316300174
[22] R. Skelton, F. Fraternali, G. Carpentieri, and A. Micheletti, "Minimum mass design of tensegrity bridges with parametric architecture and multiscale complexity," *Mechanics Research Communications*, vol. 58, pp. 124–132, 2014.
[23] A. Yeshmukhametov and K. Koganezawa, "A simplified kinematics and kinetics formulation for prismatic tensegrity robots: Simulation and experiments," *Robotics*, vol. 12, no. 2, p. 56, 2023.